Equilibrium Swelling and Kinetics of pH-Responsive Hydrogels: Models, Experiments, and Simulations

Sudipto K. De, N. R. Aluru, *Member, IEEE*, B. Johnson, W. C. Crone, David J. Beebe, *Member, IEEE*, and J. Moore

***Abstract*—The widespread application of ionic hydrogels in a number of applications like control of microfluidic flow, development of muscle-like actuators, filtration/separation and drug delivery makes it important to properly understand these materials. Understanding hydrogel properties is also important from the standpoint of their similarity to many biological tissues. Typically, gel size is sensitive to outer solution pH and salt concentration. In this paper, we develop models to predict the swelling/deswelling of hydrogels in buffered pH solutions. An equilibrium model has been developed to predict the degree of swelling of the hydrogel at a given pH and salt concentration in the solution. A kinetic model has been developed to predict the rate of swelling of the hydrogel when the solution pH is changed. Experiments are performed to characterize the mechanical properties of the hydrogel in different pH solutions. The degree of swelling as well as the rate of swelling of the hydrogel are also studied through experiments. The simulations are compared with experimental results and the models are found to predict the swelling/deswelling processes accurately. The validated models are then used to study the influence of the various hydrogel and solution parameters on the degree and rate of swelling/deswelling of the hydrogel. [785]**

***Index Terms*—Hydrogels, kinetics, material properties, mathematical models, pH-sensitive gels, simulation.**

I. Introduction

HYDROGELS are networked structures of polymer chains crosslinked to each other and surrounded by an aqueous solution. The polymer chains contain acidic or basic groups bound to them. The acidic groups on the chains deprotonate at high pH, whereas the basic groups protonate at low pH. In the presence of an aqueous solution, the polymer chains absorb water and the association, dissociation and binding of various ions to polymer chains causes the hydrogel to swell. The swelling and shrinking properties of hydrogels are currently being exploited in a number of applications including control of microfluidic flow [1], muscle-like actuators [2], [3], filtration/separation [4], and drug delivery [5], [6]. The structure and properties of hydrogels are similar to many biological tissues such as cartilage and the corneal stroma in the eye [7], [8]. Even though a number of applications are currently being pursued using hydrogels, very little is known about the mechanical behavior or the theoretical models that describe the various physical processes in hydrogels.

Manuscript received December 4, 2001; revised March 4, 2002. This work was supported by DARPA, AFRL, Air Force Command, and USAF under Agreement F30602-00-1-0570. Subject Editor H. Fujita.

S. K. De, N. R. Aluru, and J. Moore are with the Beckman Institute for Advanced Science and Technology, University of Illinois at Urbana-Champaign, Urbana, IL 61801 USA.

B. Johnson, W. C. Crone, and D. J. Beebe are with the University of Wisconsin at Madison, Madison, WI USA.

Digital Object Identifier 10.1109/JMEMS.2002.803281.

Thermodynamic models have been used extensively to explain the equilibrium swelling of hydrogels. These models are simple to use, but they do not provide good quantitative results [9], [10]. Many of the input parameters in the thermodynamic model are difficult to determine and are often adjusted to "fit" the model to the gel's equilibrium behavior. Theoretical models have been developed to predict the swelling and deswelling kinetics of hydrogels [11], [12]. However, the models and experiments were done under nonbuffered solution conditions, where the swelling rate is very slow. Prior studies have also dealt with the mechanical properties of the hydrogel [13]–[15]. However, they have not been extensive and the dependence of mechanical properties on various physical parameters is still an active area of research. The focus of this paper is to enhance our current understanding on the mechanical properties as well as on the theoretical models that describe the various physical processes in hydrogels.

A. Hydrogel Basics: Structure and Properties

Ionic polymer gels are composed of a solid and a liquid phase [16]. The solid portion of the gel consists of a crosslinked polymer network with acidic or basic groups bound to the polymer chains. When immersed in a suitable solvent, the chains in the network become solvated. Crosslinks prevent complete mixing of the polymer chains and the solvent by providing an elastic restoring force that counters the expansion of the network. A gel is the combination of the polymer network and the internal solution that surrounds the chains as shown in Fig. 1. As indicated by Fig. 1, not all ionizable groups (acidic or basic) become fully dissociated (protonated/deprotonated). For the pH sensitive hydrogels in this paper, acidic carboxyl groups are bound to the chains and their dissociation produces H^+ ions.

Hydrogels are capable of undergoing large reversible deformations in response to changes in several environmental factors [17]. For example, hydrogel size is sensitive to solution pH, salt concentration, temperature, and electric fields. Special modification of the polymer's structure can also lead to gels that are sensitive to specific biological agents [18].

B. The Hydrogel Swelling/Deswelling Phenomena

For a hydrogel containing acidic groups bound to their polymer chains, the H^+ comes off in basic solutions and combines with OH^- to form H_2O. Charge is compensated by cations that enter the gel together with another OH^-. Charge neutrality is maintained. The increased cation concentration gives rise to an osmotic pressure that causes the gel to swell/deswell. Ionic gels also swell/deswell due to the general tendency of the polymer network to mix with the solution,

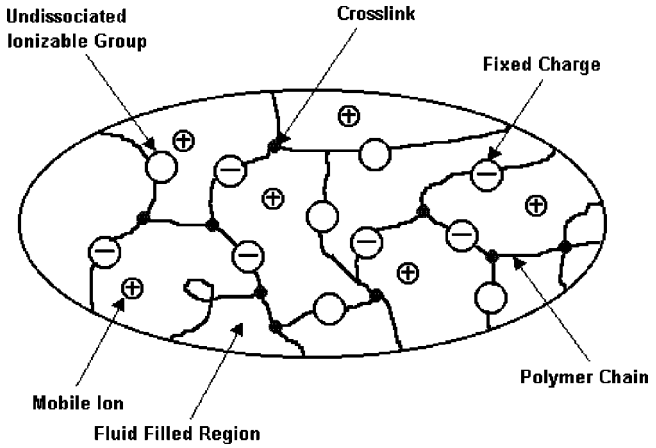

Fig. 1. Structure of a hydrogel.

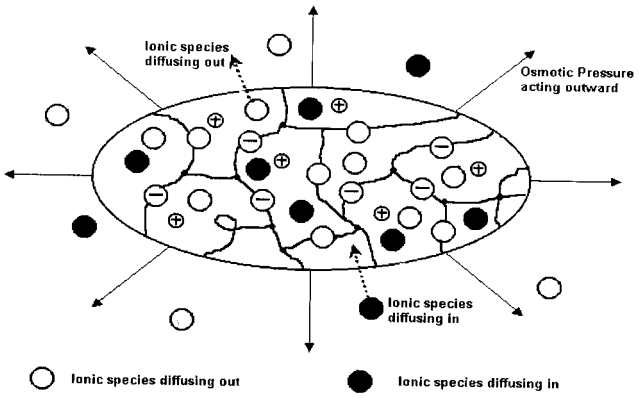

Fig. 2. The swelling phenomena of a hydrogel in a buffered pH solution.

but, typically the osmotic force is much greater than the mixing force. Equilibrium of ionic gels occurs when the elastic restoring force of the network balances the osmotic forces.

Free swelling experiments with gels indicate that they swell faster in the presence of buffered solutions [10], [11]. The conjugate base of the buffer reversibly binds hydrogen ions in regions of higher concentration and releases the hydrogen ion after diffusing to a region of lower concentration [10]. This provides an additional path for the diffusion of H^+. The higher the concentration of buffer, the more is the amount of H^+ reversibly bound to the buffer ion and hence more is the amount of H^+ delivered. For the gels considered in this paper, the buffer concentration inside the gel is significantly higher than that of H^+, hence the amount of H^+ delivered by buffer is much more than that by diffusion of free H^+, although buffers diffuse much more slowly when compared to free H^+. There is an apparent diffusion rate measured for H^+ which is several times higher than the diffusion coefficient of H^+ alone [19]. Fig. 2 shows the swelling process, where a change in the outside pH causes a concentration difference between the inside and outside of the gel. Some ions diffuse into the gel while others diffuse out of the hydrogel. The osmotic pressure inside the gel is higher than outside and hence acts in the outward direction during swelling.

C. Application of Hydrogels in MEMS

The sensitivity of hydrogels to a large number of physical factors like temperature [17] , light [9], electrical voltage [5], pH and salt concentration [5] make them candidates for a broad range of applications. Their comparatively large volume changes and large force exertion combined with favorable scaling of their time response make them very suitable for application as microsensors and microactuators in MEMS devices. Because their response is typically diffusion driven, scaling to micro dimensions enhances the time response such that response times of seconds are practical. Hydrogels can be used as valves to regulate the flow of fluids [1], [23] in microchannels. Hydrogel-actuated microvalves that respond to changes in the concentration of specific chemical species in an external liquid environment have also been fabricated and tested [24].

D. Present Work

Equilibrium hydrogel swelling has been explained earlier by using thermodynamic models [20], which are good from a qualitative point of view, but not from a quantitative point of view as they involve a number of fitting parameters. In this paper, the equilibrium swelling/deswelling process has been modeled using the steady-state Nernst–Planck equation, the Poisson equation and the mechanical equilibrium equation [21], [22]. The equilibrium model takes into account the hydrogen ion and salt concentrations of the solution. The effect of the buffer ions is not considered in the equilibrium model as they affect only the rate of diffusion but not the final equilibrium state.

A nonlinear coupled chemical diffusion equation and a mechanical equation have also been developed to predict gel swelling/deswelling kinetics. Modeling gel kinetics requires an accurate description of the diffusion of hydrogen ions into and out of the gel. This requires taking into account the chemical reactions of the hydrogen ions with the fixed charge groups and buffer's effect on hydrogen ion diffusion as well as the forces and flow of fluids inside the membrane. The model developed here modifies Grimshaw's [11] model for hydrogel kinetics to include the influence of pH buffer in the solution. Results from the numerical model are compared to experimental swelling and deswelling experiments performed on a cylindrical hydrogel.

The rest of the paper is outlined as follows: Section II describes the theory of the equilibrium and the kinetic models, Section III describes the experiments performed for material characterization and model validation, Section IV shows results comparing simulations with experimental data and conclusions are presented in Section V.

II. Theory

A cylindrical hydrogel in a channel is considered as shown in Fig. 3. The displacement of the top and the bottom surfaces of the gel are restricted by the glass channel. It is reasonable to assume that the hydrogel deforms only in the radial direction. As a result, the swelling/deswelling of the gel can be modeled by considering only a circular section as shown in Fig. 3. A one-dimensional model can be applied along the diameter of the circular cross section to investigate the swelling behavior of the hydrogel.

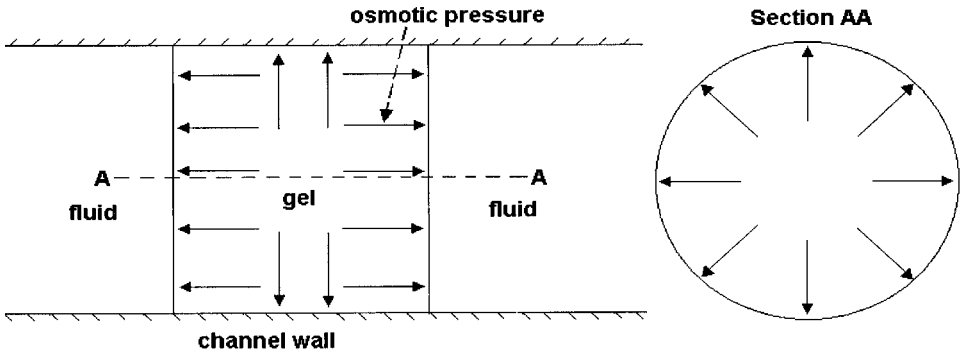

Fig. 3. A cylindrical hydrogel in a channel. Channel walls are assumed to be rigid constraints. The cross section of the cylinder shown in section AA depicts the gel under radial osmotic pressure.

A. Equilibrium Model

A one-dimensional model has been developed for predicting the equilibrium deformation of a hydrogel immersed in a given pH solution with known salt concentrations. A Nernst–Planck equation coupled with the Poisson and the mechanical equilibrium equation can be used to calculate the ionic concentration, electric potential and the hydrogel swelling. In the mechanical equation, the stress arising due to electrostatic interaction among the ions has been neglected as in the absence of an applied electric field it is very small [28]. The Nernst–Planck equation [21] is given by

$$\overline{D}_k \frac{\partial^2 c_k}{\partial x^2} + \mu_k z_k \frac{\partial c_k}{\partial x}\frac{\partial \psi}{\partial x} + \mu_k z_k c_k \frac{\partial^2 \psi}{\partial x^2} = 0 \qquad (k = 1, 2, 3, \ldots, N) \quad (1)$$

where $\overline{D}_k$ is the effective diffusivity of the kth ion inside the hydrogel, c_k is the concentration of the kth ionic species inside the hydrogel, μ_k is the ionic mobility and z_k is the valency of the kth ion, the index $k = 1, 2, 3, \ldots, N$ describes the N ionic species present in the solution. ψ is the electric potential and F is the Faraday constant. The Einstein relationship [29] relates diffusivity to ionic mobility, i.e.,

$$\overline{D}_k = \frac{\mu_k RT}{F} \quad (2)$$

where R is the universal gas constant and T is the absolute temperature. The Poisson equation [21] is given by

$$\frac{\partial^2 \psi}{\partial x^2} = -\frac{F}{\epsilon \epsilon_0}\left(\sum_{k=1}^{N} z_k c_k + z_f c_f\right) \quad (3)$$

where ϵ_0 is the dielectric constant of vacuum and ϵ is the relative dielectric constant of the solvent. The quantities z_f and c_f are the valency and concentration of the fixed charge in the hydrogel.

The osmotic pressure, P_{osmotic}, is calculated by the following equation:

$$P_{\text{osmotic}} = RT\sum_{k=1}^{N}\left(c_k - c_k^0\right) \quad (4)$$

where c_k^0 is the concentration of the kth ion in the stress-free state in the outside solution.

The mechanical equilibrium equation based on Biot's Theory [30], balances the stress generated in the hydrogel with the osmotic pressure. The mechanical equilibrium equation is given by

$$\nabla . \sigma = 0 \quad (5)$$

where σ is the stress tensor. For the circular gel cross-section subjected to osmotic pressure (shown in Fig. 3) an analytical solution can be developed [22]

$$u(r) = \frac{P_{\text{osmotic}}(1+\nu)(1-2\nu)r}{E} \quad (6)$$

where $u(r)$ is the displacement at a distance r in the radial direction, ν is the Poisson's ratio and E is the Young's Modulus of the hydrogel.

When the hydrogel geometry changes because of the osmotic pressure, the fixed charge concentration inside the hydrogel changes. The fixed charge concentration appears in the Poisson equation and is related to the hydrogel volume change by

$$c_f = \frac{1}{H}\frac{c_{mo}^s K}{(K + c_H)} \quad (7)$$

where H is the local hydration state of the gel, K is the dissociation constant of the fixed charge group, c_{mo}^s is the total concentration of ionizable groups in the gel before swelling and c_H is the concentration of hydrogen ion. Hydration is defined as the ratio of the volume of fluid to the volume of solid inside the gel and is equal to ϵ_r (strain in the radial direction) for the circular cross-section. The radial strain ϵ_r is related to $u(r)$ as follows:

$$\epsilon_r = \frac{\partial u(r)}{\partial r}. \quad (8)$$

Since equations (1), (3) and (5) are coupled, a self-consistent solution is computed by iteratively solving the Nernst–Planck, Poisson and the mechanical equilibrium equations. Numerical solution of the Nernst–Planck and the Poisson equation is accomplished by using the finite cloud method [31].

B. Kinetic Model

Swelling of ionic hydrogels induced by pH changes can be modeled by considering the diffusion of hydrogen ions [11] governed by the chemical diffusion equation along with the mechanical equation. The mechanical equation takes into account

the deformation of the polymer network that occurs during the diffusion of hydrogen ions into the gel.

1) Chemical Diffusion Equation: Following the model presented in [11], the flux of an ionic species is described by the Nernst–Planck equation which includes flux due to diffusion, electrical migration, and convection

$$\Gamma_k = \phi\left[-\overline{D}_k\,\frac{\partial c_k}{\partial x} - \mu_k\, z_k c_k\,\frac{\partial \psi}{\partial x}\right] + c_k U \tag{9}$$

where Γ_k is the flux of the kth ion, ϕ is the gel porosity and U is the area-averaged fluid velocity relative to the polymer network. Gel porosity is given by [29]

$$\phi = \frac{H}{1+H}. \tag{10}$$

Transport of ions is limited to the regions containing fluid in the gel. The presence of polymer chains, which are impenetrable to mobile ions, increases the path length an ion travels, resulting in a slower diffusion rate. The diffusion rate inside the gel can be related to the diffusion in aqueous solution through an obstruction model [29]

$$\frac{\overline{D}_k}{D_k} = \left(\frac{H}{2+H}\right)^2. \tag{11}$$

At high hydration, a large amount of fluid is present between the polymer chains, and the diffusion rate approaches that of an aqueous solution. At low hydration, there is very little fluid between the polymer chains, and the effective path length an ion must travel to circumvent polymer chains lowers the diffusion rate of the ion [29]. There are several other factors not present in this model that can affect ion transport in gels including electrostatic interactions with fixed charge groups on the polymer chains, and electrodiffusion effects that occur when there are several ionic species present in the gel system.

Continuity conditions on the divergence of each ionic flux are given by

$$\frac{\partial}{\partial t}\left(Hc_k + Hc_k^b\right) = -\frac{\partial\left(\alpha\Gamma_k\right)}{\partial X} \tag{12}$$

where c_k^b is the concentration of ion k that can reversibly bound to polymer fixed charge, X is the Lagrangian coordinate system associated with the hydrogel, and α is the total area of the hydrogel normalized to its initial area. The concentration of ion k reversibly bound to the polymer chains (c_k^b) in the presence of chemical reactions can be calculated by

$$c_k^b = \frac{c_{mo}^s}{H}\left(\frac{c_k}{K+c_k}\right). \tag{13}$$

In the presence of a neutral salt solution, H^+ ions can be considered a minority carrier of electric current, allowing the flux of H^+ ions to be uncoupled from that of other ions [11]. The H^+ concentration in a neutral salt solution (pH approximately 7) is around 10^{-7} M, where as typically the salt concentration is around 10^{-3} M. As a result, the H^+ becomes a minority carrier with a negligible effect on the electric flux [equation (3)] generated by the movement of ions. Combining equations (9), (12), and (13), a nonlinear diffusion-reaction equation for the concentration of H^+ ions in the hydrogel is obtained

$$\frac{\partial}{\partial t}\left[c_H\left(H + \frac{c_{mo}^s}{K+c_H}\right)\right] = \frac{\partial}{\partial X}\left[\alpha\phi\left(\overline{D}_H\frac{\partial c_H}{\partial x} + \mu_H z_H c_H\frac{\partial \psi}{\partial x}\right) - \alpha c_H U\right] \tag{14}$$

where $\overline{D}_H$ is the diffusion rate of hydrogen ions in the hydrogel, c_H is the internal concentration of hydrogen ions, and c_H^b is the concentration of hydrogen ions reversibly bound to the hydrogel's fixed charges.

Free swelling experiments with gels indicate that they swell faster in the presence of buffered solutions [10], [11]. The buffer's effect on the transport of hydrogen ions can be modeled by including additional terms in the continuity equation of hydrogen ions in the gel [11]

$$\frac{\partial}{\partial t}\left(Hc_H + Hc_H^b + Hc_{HB}\right) = -\frac{\partial\left(\alpha\Gamma_H + \alpha\Gamma_{HB}\right)}{\partial X}, \tag{15}$$

where c_{HB} is the concentration of hydrogen ions bound to the buffer, Γ_H is the flux of hydrogen ions, and Γ_{HB} is the flux of hydrogen ions bound to the buffer. Using a reaction isotherm, c_{HB} can be expressed in terms of c_H by

$$c_{HB} = \frac{c_T c_H}{K_B + c_H} \tag{16}$$

where K_B is the dissociation constant of the buffer and c_T is the total buffer concentration given by $c_T = c_{B^-} + c_{HB}$. The term c_{B^-} represents the internal concentration of the buffer's conjugate base. The flux of hydrogen ions in the absence of an electric field is

$$\Gamma_H = \frac{H}{1+H}\left[-\overline{D}_H\,\frac{\partial c_H}{\partial x}\right]. \tag{17}$$

The flux of the buffer is proportional to the flux of the hydrogen ions

$$\Gamma_{HB} = \frac{\overline{D}_{HB}}{\overline{D}_H}\,\frac{c_T}{K_B + c_H}\,\Gamma_H \tag{18}$$

where $\overline{D}_{HB}$ is the diffusion rate of buffer in the hydrogel. Using (16)–(18), (15) becomes

$$\frac{\partial}{\partial t}\left[Hc_H + \frac{c_{mo}^s c_H}{K+c_H} + \frac{Hc_T c_H}{K_B + c_H}\right] = \frac{\partial}{\partial X}\left[\alpha\left(\frac{H}{1+H}\right)\left(1+\frac{\overline{D}_{HB}}{\overline{D}_H}\,\frac{c_T}{K_B+c_H}\right)\left(\overline{D}_H\,\frac{\partial c_H}{\partial x}\right)\right]. \tag{19}$$

2) Mechanical Equations: Changes in membrane hydration can be calculated by mechanical equations that describe the forces and flow of fluid. A modified version of Darcy's law [29] describes fluid flow in the gel

$$U = -k'\left[\frac{\partial P}{\partial x} + z_f c_f F\,\frac{\partial \psi}{\partial x}\right] \tag{20}$$

where k' is the hydraulic permeability of the gel and P is the fluid pressure gradient. In equation (20), the first term is the fluid flow due to pressure gradient and the second term is due

to the electro-osmotic forces which has been neglected as explained earlier. Changes in hydration are subject to a continuity condition

$$\frac{\partial H}{\partial t} = -\frac{\partial(\alpha U)}{\partial X}. \tag{21}$$

Stress in the gel due to deviations from mechanical equilibrium are described by a linear elastic constitutive law

$$p(X, t) = M\epsilon \tag{22}$$

where M is the bulk modulus of the gel and ϵ is the compressive strain. Local compressive strain in the gel is given by the difference between the local hydration from an equilibrium hydration $H_{eq}(c_H)$, i.e.,

$$\epsilon = \frac{H_{eq}(c_H) - H(c_H)}{1 + H_{eq}(c_H)}. \tag{23}$$

Neglecting inertial effects, conservation of linear momentum is given by the divergence of the total stress

$$\frac{\partial(P+p)}{\partial x} = 0. \tag{24}$$

Combining equations (20)–(24) gives an expression describing the mechanical processes in the gel

$$\frac{\partial H}{\partial t} = \frac{\partial}{\partial X}\left[\alpha k'\left(-\frac{\partial(M\epsilon)}{\partial x} + z_f c_f F\frac{\partial \psi}{\partial x}\right)\right]. \tag{25}$$

III. Experiments and Model Validation

The experiments performed can be divided into two categories. One set of experiments was performed to obtain the material properties, such as Poisson's ratio and Young's modulus, needed in the models. Another set of experiments was performed to validate the models. Data were collected on equilibrium swelling and swelling kinetics of hydrogels to validate the equilibrium and kinetic models, respectively. The hydrogels used in the experiment were homogeneous copolymers of HEMA (hydroxy–ethyl–methacrylate acid) and acrylic acid with 1% of a diacrylate crosslinker. The acidic groups bound to the polymer chains are carboxyl groups which made the gels pH sensitive.

A. Materials Characterization Experiments

Fundamental mechanical experiments were conducted to determine properties needed for the governing mechanical equilibrium equation and the linear elastic constitutive law used in the models described above. Hydrogels exhibit elastomeric behavior and several mechanical properties can be determined through traditional tensile testing. However, it must be appreciated that the mechanical properties of hydrogels depend on the environmental conditions in which they are tested, as well as the deformation rate at which a mechanical test is conducted.

Tests were conducted in accordance with ASTM D 638-99 on dumbbell shaped tension samples made of pH responsive hydrogel. The standard dimensions of the dumbbell sample (Type IV) were scaled down to a gauge section width of 1 mm to better approximate the component sizes being developed in microfluidic devices. Sample geometries were created by injecting the prepolymer liquid into a polydimethylsiloxane (PDMS) mold. The mold was generated by employing the sandwich molding process previously reported in [32]. Anisotropic material behavior was avoided by exposing the monomer to PDMS walls exclusively during polymerization. Polymerization was performed in the PDMS mold using a Novacure UV source at an intensity of 15 mW/cm^2. This sample preparation technique also has the advantage of producing a very uniform rectangular cross section.

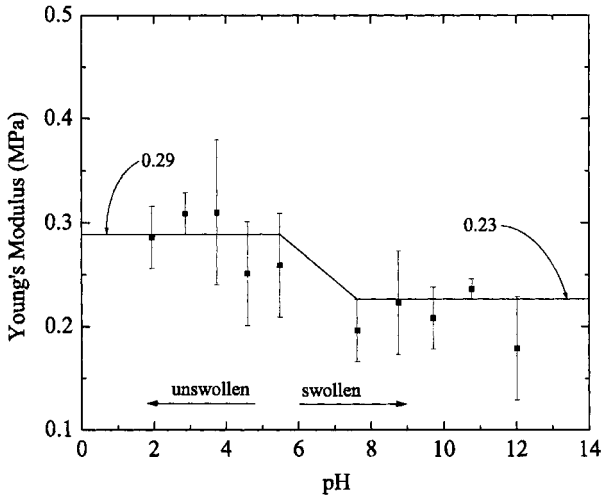

Fig. 4. Young's modulus measured in 200-μm-thick samples in the unswollen and swollen states. The average and standard deviation are shown for five samples at each pH levels.

Tensile testing was conducted with an Instron 5548 micromechancial testing machine using a 10 N load cell and an environmental chamber. An individual sample was placed in the grips and the sample/grip assembly was immersed in a pH solution surrounded by a temperature controlled bath held at 25 °C. Buffered solutions of 0.2 M ionic strength varying between pH values of 2 and 12 were made from NaH_2PO_4, NaOH, HCl, NaCl, and Na_2HPO_4. Testing was conducted in displacement control using a displacement rate of 5 mm/min.

The initial slope of the stress/strain curve was used to identify the Young's modulus, E, at different pH levels. At low pH, prior to swelling, the hydrogel has an average Young's modulus near 0.29 MPa; whereas at high pH, after swelling, E decreases to 0.23 MPa. The experimental values were fit with a tri-linear function assuming a linear transition in modulus with pH between pH values of 5.5 and 7.5. From the experimental data, in between pH 5.5 to 7.5, the hydrogel undergoes a major phase change and it does not undergo any phase change before pH 5.5 or after pH 7.5. Hence, it is quite reasonable to assume E to remain in constant before pH 5.5 and after pH 7.5, in between them, a linear fit is assumed for convenience (see Fig. 4).

Tension samples used in the determination of Poisson's ratio were polymerized with a random array of uncoated 30-μm-glass beads (Polysciences, Inc.) and were tested in displacement control at a rate of 2 mm/min. Since the beads occupy less than 0.01% of the sample volume, it is assumed that they have no significant effect on the macroscopic material properties. Sequential images were captured in 1.6-s intervals throughout testing with a digital camera (SPOT RT Color, Diagnostic Instruments, Inc.) equipped with a 200-mm zoom lens. Testing

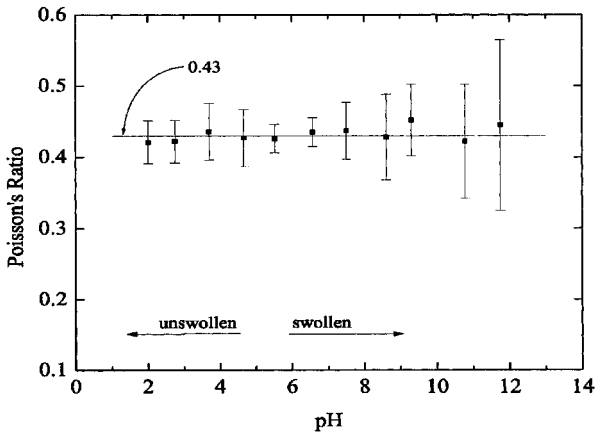

Fig. 5. Poisson's ratio measured in 500-μm-thick samples in the unswollen and swollen states. The average and standard deviation are shown for five samples at each pH level.

was conducted in the environmental chamber described above and a cylindrical lens was placed in the optical path to remove distortion caused by the chamber. Image analysis software (Metamorph 4.6r6, Universal Imaging Corporation) was used to track the positions of individual beads for strain calculations.

The ASTM D-638-99 method using an averaged value based on engineering strains was employed to calculate Poisson's ratio. This method uses the slope of the transverse strain versus the axial strain

$$\nu = -\frac{de_{\text{trans}}}{de_{\text{axial}}}. \tag{26}$$

Linear regression analysis shows that there is a small variation of Poisson's ratio with pH. The average value of the Poisson ratio is found to be 0.43. The error in the Poisson's ratio value ranges from ± 0.02 at pH $= 5.5$ to ± 0.12 at pH $= 11.8$. The values of Poisson's ratio chosen for the simulation lie within the error ranges in the measurements. It should be noted that the gel is in its unswollen state after polymerization; subsequently, a cavity is formed around the embedded beads upon swelling. Movement of the beads within the cavity provides a possible explanation for the systematic increase in error observed with increasing pH (see Fig. 5).

The Lame coefficient, λ, and the shear modulus, γ, used in the equilibrium model were calculated from experimental values of Young's modulus, E, and Poisson's ratio, ν, using

$$\lambda = \frac{\nu E}{(1+\nu)(1-2\nu)} \tag{27}$$

and

$$\gamma = \frac{E}{2(1+\nu)}. \tag{28}$$

Similarly, the bulk modulus, M, incorporated in the constitutive law used in the kinetic model was calculated from experimental values using:

$$M = \frac{E}{3(1-2\nu)}. \tag{29}$$

TABLE I
CYLINDRICAL HYDROGEL PROPERTIES

$\bar{D}_H$	9.3 x $10^{-9}\frac{m^2}{s}$	K	$10^{-2.0}$ mM
$\bar{D}_{H_2PO_4}$	8.79 x $10^{-10}\frac{m^2}{s}$	$K_{H_2PO_4}$	6.2 x 10^{-5} mM
c^s_{mo}	1800 mM	ν	0.43
M	0.61 Mpa	k'	2.2 x $10^{-16}\frac{m^4}{Ns}$

The material properties and other constants used for the simulations are given in Table I. The text book value [33] for K (dissociation constant for the carboxylic acid group) is $10^{-2.1}$ mM. However, it decreases with the increase in solution pH [34] and so a constant value of $10^{-2.0}$ mM has been chosen for all gels.

B. Model Validation Experiments

Using the experimentally determined materials properties described in the previous section and a fixed charge density, c^s_{mo}, of 1800 mM, the models are compared to both equilibrium and kinetic validation experiments.

1) Experimental Setup: A scheme of the experimental setup is shown in Fig. 3. Cylindrical gels were fabricated using photopolymerization techniques within microchannels.

The rectangular cross section of the micro-channel was approximately 1000 μm wide by 180 μm high. The micro-channel restricts the hydrogel from expanding in the height direction and only allows swelling in the radial direction. This constraint allows swelling and deswelling to be modeled as a one-dimensional diffusion problem along the hydrogel's diameter. Because the micro-channel constrains the hydrogel's height, the volume of the hydrogel is only a function of diameter.

2) Equilibrium Experiments: The equilibrium behavior of hydrogel was characterized by varying the pH of the solution and by measuring the equilibrium diameter of the cylinder using a microscope with a built-in ruler. The diameter of the hydrogel for different pH solutions was recorded. The ionic strength of the solution was 0.3 M and the buffer was phosphoric acid. Experiments were performed for gels of different diameters (300 μm, 400 μm, 500 μm, 700 μm) for pH variations from 2 to 12.

3) Kinetic Experiments: The dynamic behavior of hydrogels was also recorded. Experiments were done for gels of diameter 150 μm, 200 μm and 300 μm for pH variations from 3 to 6. Initially, the gels were equilibrated in a buffer solution of pH $= 3.0$. The solution was then flushed and replaced with a solution of pH $= 6.0$. In the presence of the new solution, the gels began to swell toward their new equilibrium diameters. The ionic strength of the solution was 0.2 M with phosphoric acid as buffer. Measurements of the gel diameters were taken during the course of the experiments using a Sony CCD camera. The experiments were stopped after the gels reached their equilibrium hydrations. Deswelling experiments were performed by returning the bath solution to a pH of 3.0 and recording the gel diameters at various times. Several separate swelling and deswelling experiments were performed for each hydrogel. Some experiments were done on a 400 -μm gel under the similar conditions but for different ranges of pH namely, 3.8 to 4.67, 4.67 to 5.67,

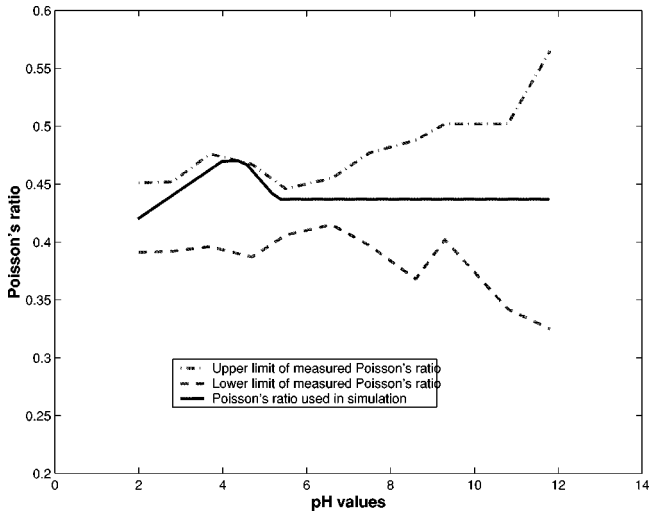

Fig. 6. Poisson's ratio used for simulation of hydrogel swelling.

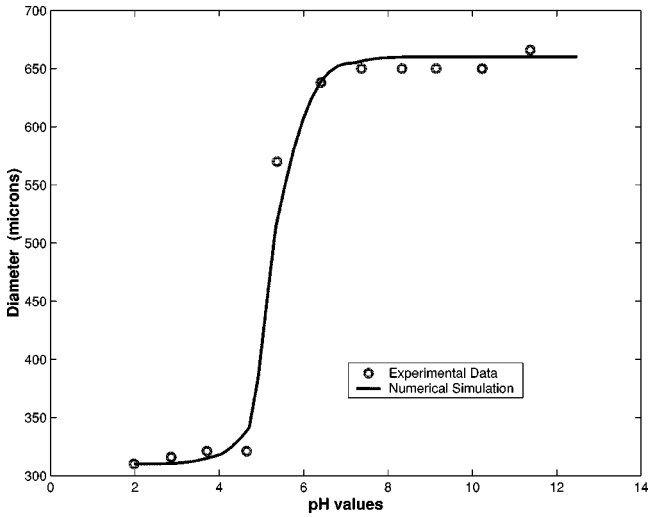

Fig. 7. Experiment versus simulation for 300 μm hydrogels.

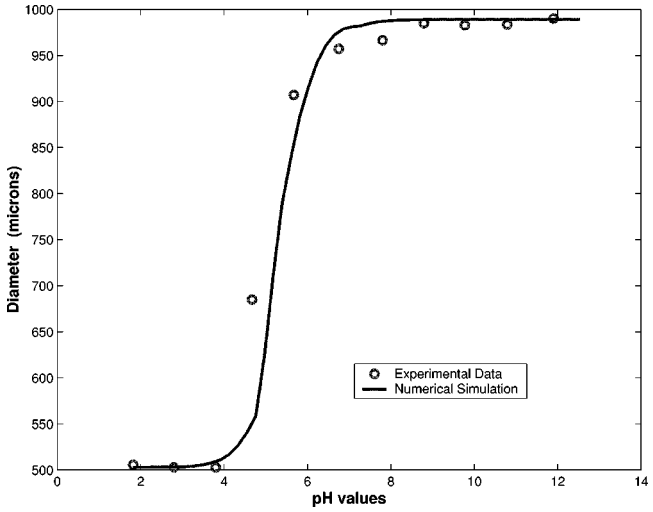

Fig. 8. Experiment versus simulation for 400 μm hydrogels.

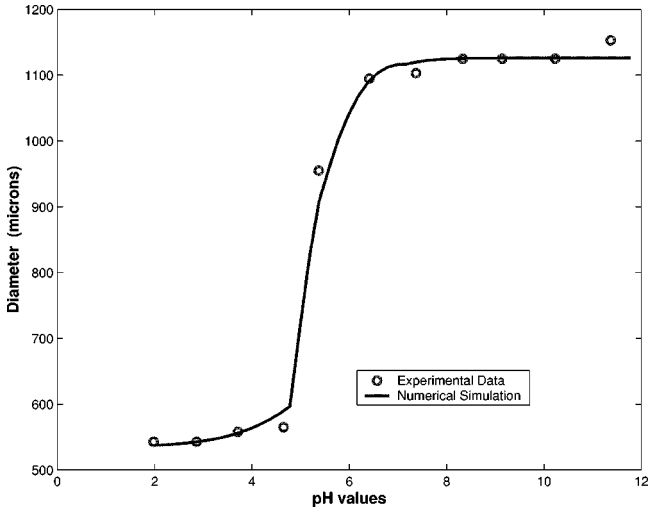

Fig. 9. Experiment versus simulation for 500 μm hydrogels.

and 6.75 to 7.8. The ionic strength of the solution here was 0.3 M. The gel diameters were converted to hydration values using the relation

$$H = \frac{V_f}{V_s} = \frac{\pi d^2 h - \pi d_0^2 h}{\pi d_0^2 h} = \frac{d^2 - d_0^2}{d_0^2} \tag{30}$$

where d and d_0 are the deformed and undeformed diameter of the hydrogel.

IV. Results

A. Equilibrium Results

Due to symmetry, half of the gel diameter (from the center to the edge) is considered in the computational domain. A thin boundary layer is considered on the gel-solution edge, where a linear variation was assumed for the fixed charge concentration varying from c_f inside the gel to 0 outside the gel. Symmetric boundary conditions are applied at the gel end of the domain and Dirichlet boundary conditions are applied at the solution end.

As discussed in Section III-A, the materials properties were determined experimentally and used in the equilibrium model for the hydrogels. For pH less than 5.5, a Young's modulus of 0.29 MPa is used. For pH greater than 7.5, a Young's modulus of 0.23 MPa is used. For pH between 5.5 and 7.5, the Young's modulus is assumed to vary linearly. The value of Poisson's ratio used in the simulations is within the experimental ranges. At low pH, prior to swelling, a value of 0.420 is used in the model, and a higher value of 0.470 is used around pH 4 and 5 which is within the experimental range. At high pH a Poisson's ratio of 0.437 is used as shown in Fig. 6. The same mechanical properties are used for all gels. A fixed charge density of $c_{mo}^s = 1800$ mM is used.

Figs. 7–10 show the comparison between experimental results and simulations for cylindrical gels of different diameters when pH changes from 2 to 12.

The simulations match closely with the experimental results which proves that a chemoelectromechanical model can satisfactorily explain the hydrogel swelling process. The 400-μm gel was photopolymerized with a different microscope for a different time length as compared to the others. The extent of polymerization will depend on light intensity which will vary from

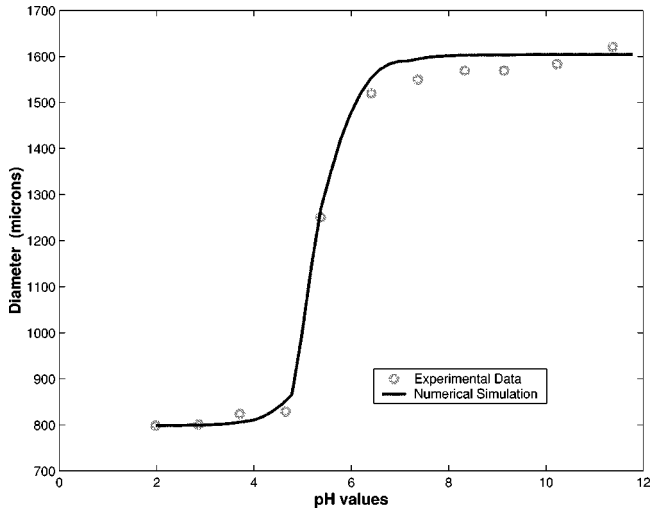

Fig. 10. Experiment versus simulation for 700 μm hydrogels.

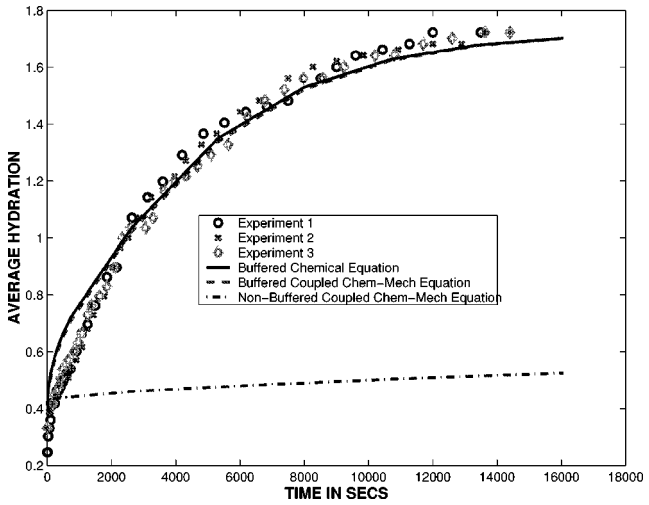

Fig. 11. Experiment versus simulation for a 300-μm gel for a pH change of 3 to 6.

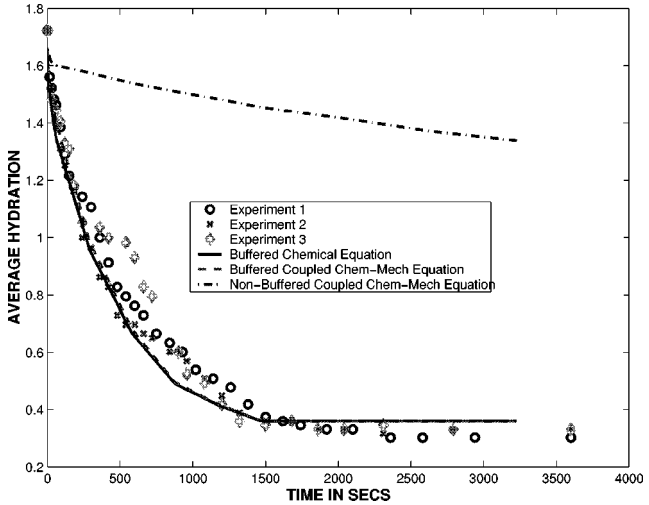

Fig. 12. Experiment versus simulation for a 300-μm gel for a pH change of 6 to 3.

one microscope to another. As a result, the crosslinking density of this gel is expected to be different from that of other gels and hence the Poisson ratio can also be different from that of other gels. This explains why the simulation for the 400-μm gel does not match very well with the experiments, since mechanical properties were assumed to be same for all gels.

B. Kinetic Results

For swelling analysis, simulations were started by setting all points in the gel in equilibrium with the solution pH (e.g., pH $=$ 3). Using Donnan partitioning theory [11], initial concentrations inside the gel are computed. The hydration values for the given pH are taken from the equilibrium results. At time $t_1 = 0$, the solution pH was changed to the final pH (e.g., pH $= 6$), and H and c_H values at the boundary were adjusted to reflect equilibrium with the new solution. A normalized version of (19) was incremented in time according to the algorithm given in [35]. Hydration was considered to be constant over a single time step. After finding c_H^{t+1}, H^{t+1} can be updated using the equilibrium model. A normalized version of equation (25) was then solved to modify H^{t+1} accounting for membrane mechanics. Deswelling simulations were conducted in a similar manner, except that the initial and final pH values were interchanged. Numerical swelling/deswelling was also performed in the absence of buffer (i.e., $c_T = 0$). The results show the dramatic effect buffers can have on gel kinetics.

Comparisons between numerical swelling and deswelling and experimental results are given in Figs. 11–18.

The above comparisons show that the simulated hydrogel kinetics match quite well with the experimental data. The model can predict kinetics of bigger gels more accurately as compared to smaller gels. The effect of the mechanical equations on the kinetics is found to be insignificant, hence it can be concluded that hydrogel swelling kinetics is a diffusion limited process.

C. Influence of Various Physical Parameters

As discussed in Section I-C, hydrogels can be used as sensors of different stimuli varying from chemical, biological to electrical current. Hydrogels have also been investigated as micro actuators [24] due to their large deformations and the large forces they can exert. Faster response time and more sensitivity are the essential features of a good micro actuator. In this section we exploit the controllable physical parameters of a hydrogel to achieve the above mentioned qualities of a good actuator. For hydrogels this is equivalent to faster swelling/deswelling process and larger degree of swelling/deswelling for the same stimuli.

The results in Sections IV-A and IV-B suggest that the equilibrium and the kinetic models do a reasonably good job in predicting the hydrogel swelling/deswelling processes. These models can be used to predict the influences of various physical parameters (such as fixed charge, ionic strength, diffusivity, etc.) on the swelling/deswelling processes.

1) Equilibrium Swelling: The effect of fixed charge density on the degree of swelling is first studied. The effect of fixed charge density on the Poisson's ratio of the gel is negligible [13]. However, the shear modulus is found to vary linearly with the monomer concentration and hence the fixed charge of the gel

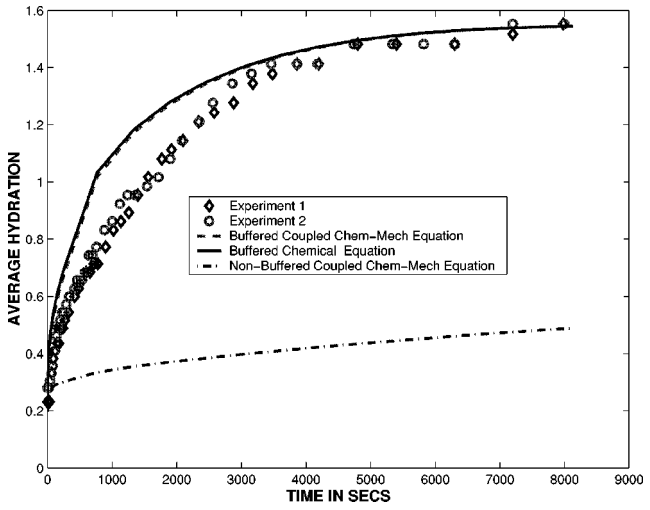

Fig. 13. Experiment versus simulation for a 200-μm gel for a pH change of 3 to 6.

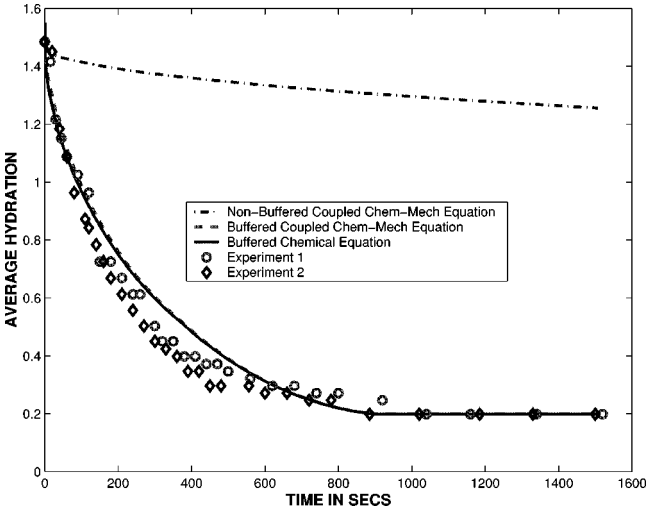

Fig. 14. Experiment versus simulation for a 200-μm gel for a pH change of 6 to 3.

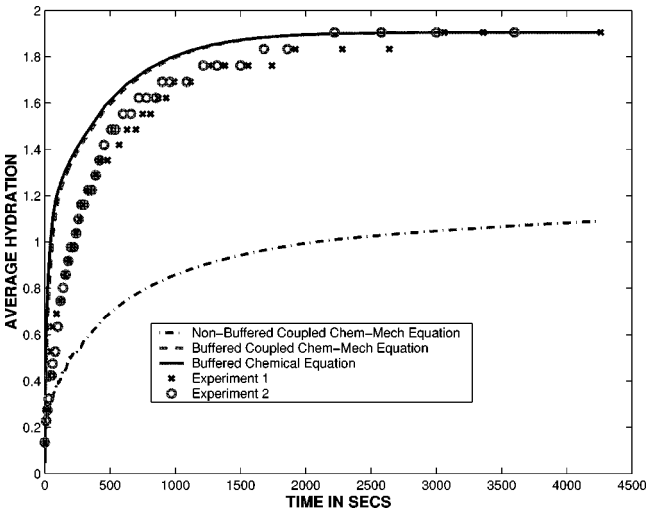

Fig. 15. Experiment versus simulation for a 150-μm gel for a pH change of 3 to 6.

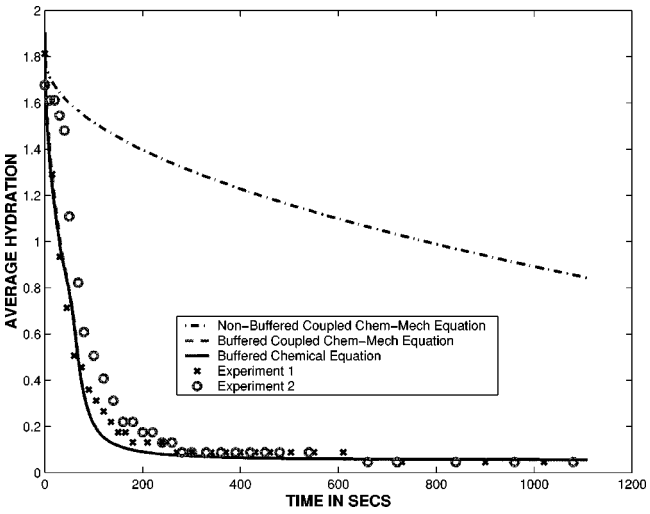

Fig. 16. Experiment versus simulation for a 150-μm gel for a pH change of 6 to 3.

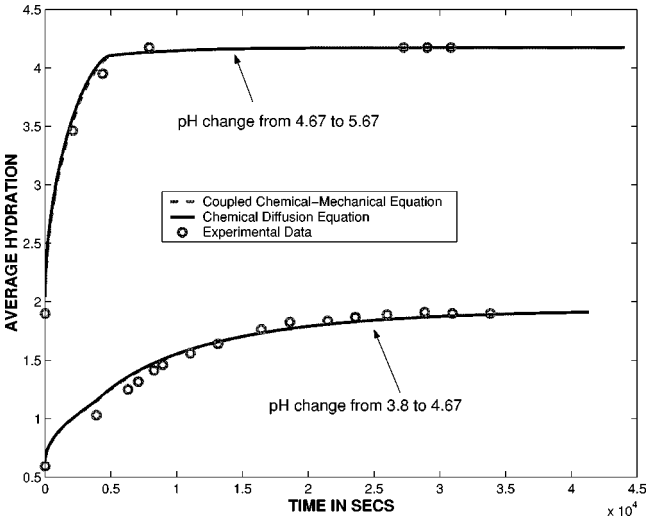

Fig. 17. Experiment versus simulation for a 400-μm gel for different pH changes.

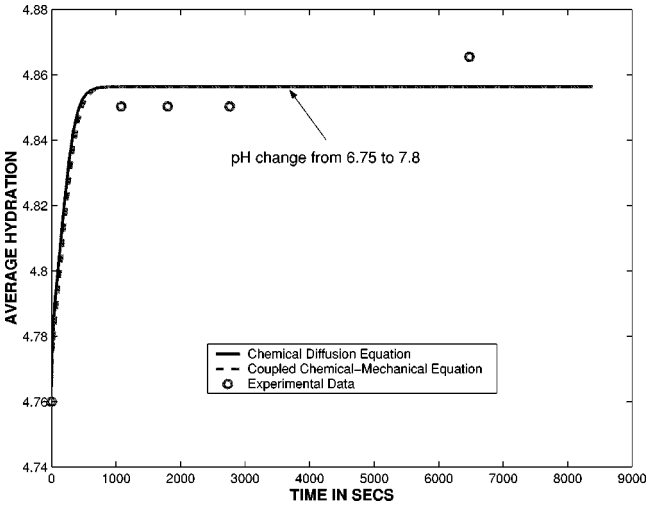

Fig. 18. Experiment versus simulation for a 400-μm gel for different pH changes.

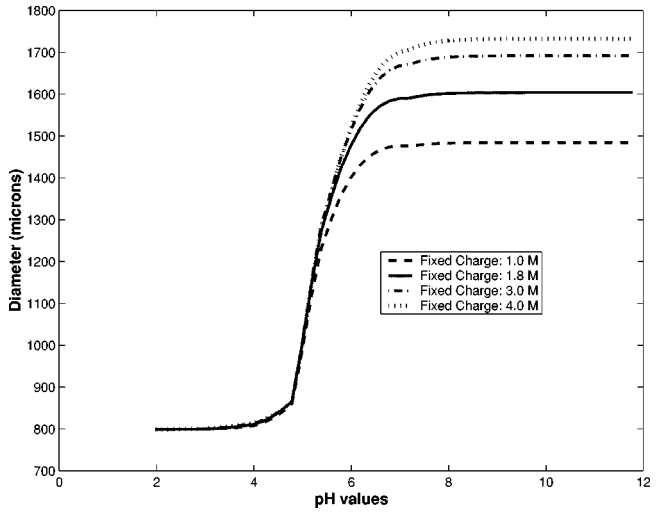

Fig. 19. Variation in equilibrium swelling of a 700-μm gel with fixed charge density.

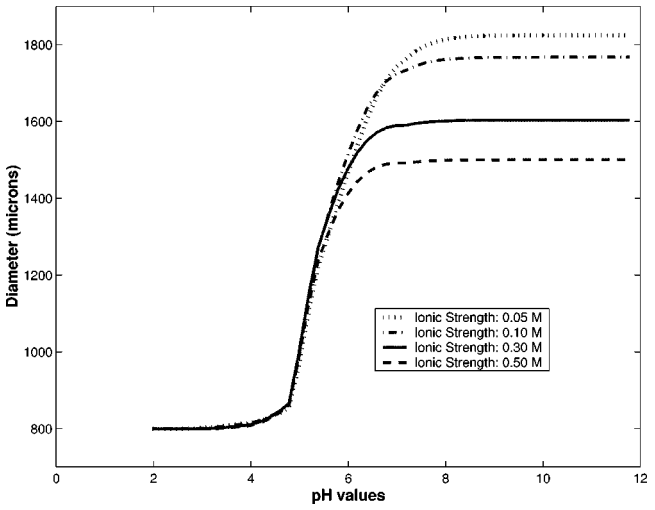

Fig. 20. Variation in equilibrium swelling of a 700-μm gel with ionic strength of the solution.

[14]. Hence, the Young's modulus also varies linearly with fixed charge as the Poisson's ratio remains constant. These changes have been taken into account in the simulation by the following equation:

$$G_0 = \frac{c_0}{N} kT \tag{31}$$

where G_0, c_0, N, k and T are the shear modulus at preparation stage, monomer concentration at preparation stage, number of monomers in a gel strand, Boltzman constant and the absolute temperature, respectively. The influence of the fixed charge density on hydrogel swelling is shown in Fig. 19. Observe that as fixed charge density increases, the degree of swelling increases at larger pH.

Next, the effect of ionic strength on the degree of swelling is studied. Poisson's ratio of the gel increases approximately linearly with the decrease in the ionic strength of the solution [15]. The shear modulus at preparation is independent of the ionic strength of the solution [see equation (31)]. Assuming that the change in Poisson's ratio is small with ionic strength, the influence of ionic strength on the degree of swelling is shown in Fig. 20. Observe that as the ionic strength decreases, the degree of swelling increases at larger pH.

Hence, for better sensitivity of hydrogels in microactuation, the fixed charge density should be kept high and the ambient ionic strength be kept low.

2) Swelling Kinetics: The buffer plays a very important role in the rate of diffusion of ions into the hydrogel. Proper selection of buffer can further increase the rate of swelling. Figs. 21 and 22 show the effect of the diffusivity of buffer ions and the concentration of buffer ions, respectively, on the rate of swelling for the 300 μm hydrogel.

Higher buffer diffusivity and concentration is found to decrease the time taken to reach equilibrium in a nonlinear manner. Hence a buffer with higher diffusivity and higher dissociation constant (which determines the concentration of the buffer for a given pH) accelerates the swelling rate. Thus for quicker time response in hydrogel actuation, the buffer in the ambient solution should be chosen such that it has higher diffusivity and higher dissociation constant.

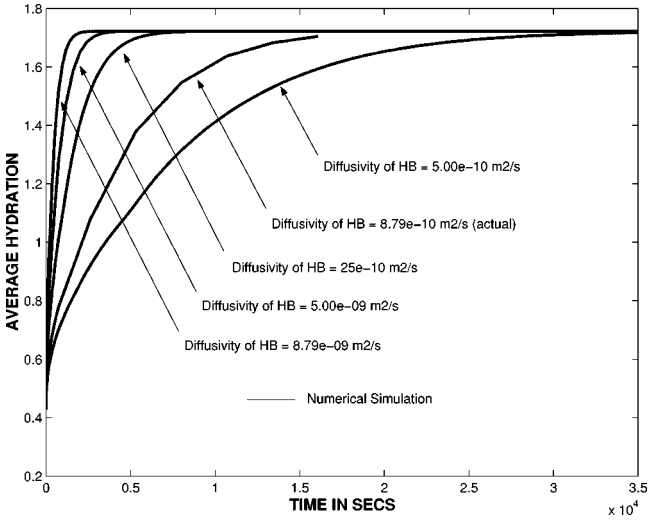

Fig. 21. Variation in swelling kinetics with buffer diffusivity.

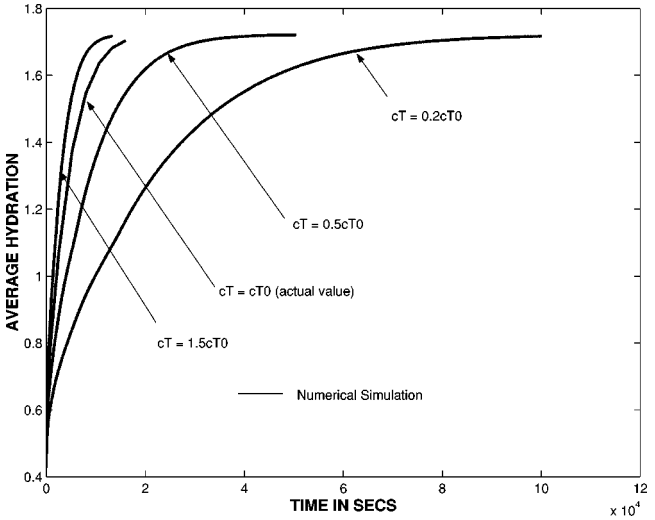

Fig. 22. Variation in swelling kinetics with buffer concentration.

V. Conclusion

An equilibrium model and a kinetic model have been developed to model the equilibrium swelling and kinetics of hydrogels. Both models do a reasonably good job in describing the swelling phenomena of hydrogels. The swelling process of hydrogels is essentially described by a chemoelectromechanical model. The swelling kinetics of hydrogels is a diffusion limited process. The average hydration during the initial time periods has been overestimated for all gels. This is more pronounced for smaller gels. The overestimation of hydration possibly suggests that electrostatic interactions and convective transfer of ions could be important and cannot be neglected for smaller gels. The influence of various physical parameters on the degree of swelling is investigated. Specifically, by increasing the fixed charge or by lowering the ionic strength of the solution, the degree of swelling can be improved. Higher buffer diffusivity and concentration can lead to faster kinetics. All these criteria can be used to enhance the performance of hydrogel microactuators such as micro-valves, chemical sensors, and other devices. Experimental data suggests that the Young's modulus of the hydrogel can change considerably with the solution pH. The Poisson's ratio is not found to vary significantly with the solution pH.

Acknowledgment

The authors would like to thank R. Ohs, J. Bauer, and Q. Yu for helpful discussions.

References

[1] D. J. Beebe, J. Moore, J. M. Bauer, Q. Yu, R. H. Liu, C. Devadoss, and B. H. Jo, "Functional hydrogel structures for autonomous flow control inside micro-fluidic channels," *Nature*, vol. 404, Apr. 2000.

[2] M. Shahinpoor, "Micro-electro-mechanics of ionic polymer gels as electrically controllable artificial muscles," *J. Intell. Mater. Syst. Struct.*, vol. 6, pp. 307–314, 1995.

[3] D. Brock and W. Lee, "A dynamic model of a linear actuator based on polymer hydrogel," *J. Intell. Mater. Syst. Struct.*, vol. 5, pp. 764–771, 1994.

[4] F. Helfferich, *Ion Exchange*, New York: McGraw-Hill, 1962.

[5] A. J. Grodzinsky and P. E. Grimshaw, "Electrically and chemically controlled hydrogels for drug delivery," *Pulsed and Self-Regulated Drug Delivery*, pp. 47–64, 1990.

[6] N. A. Peppas and L. Brannon-Peppas, "Solute and penetrant diffusion in swellable polymers. IX. The mechanism of drug release from pH-sensitive swelling-controlled systems," *J. Control. Release*, pp. 267–274, 1989.

[7] S. R. Eisenberg, "The kinetics of chemically induced nonequilibrium swelling of articular cartilage and corneal stroma," *J. Biomed. Eng.*, vol. 109, pp. 79–89, 1987.

[8] E. R. Myers, W. M. Lai, and V. C. Mow, "A continuum theory and an experiment for the ion-induced swelling behavior of articular cartilage," *J. Biomed. Eng.*, pp. 151–158, 1984.

[9] R. A. Siegel, "pH sensitive gels: Swelling equilibria, kinetics and application for drug delivery," *Pulsed and Self-Regulated Drug Delivery*, pp. 129–155, 1990.

[10] Y. Chu, P. P. Varanasi, M. J. McGlade, and S. Varanasi, "pH-induced swelling kinetics of polyelectrolyte hydrogels," *J. Appl. Polymer Sci.*, vol. 58, pp. 2161–2176, 1995.

[11] P. E. Grimshaw, Ph.D. dissertation, M.I.T., Dep. Elec. Eng. Comput. Sci., 1990.

[12] C. Wang, Y. Li, and Z. Hu, "Swelling kinetics of polymer gels," *Macromolecules*, vol. 30, pp. 4727–4732, 1997.

[13] K. Urayama, T. Takigawa, and T. Masuda, "Poisson ratio of poly (vinyl alcohol) gels," *Macromolecules*, vol. 26, pp. 3092–3096, 1993.

[14] M. Rubinstein and R. H. Colby, "Elastic modulus and equilibrium swelling of polyelectrolyte gels," *Macromolecules*, vol. 29, pp. 398–406, 1996.

[15] C. Li, Z. Hu, and Y. Li, "Poisson's ratio in polymer gels near the phase transition point," *Physic. Rev. E*, vol. 48, no. 1, 1993.

[16] O. Coussy, *Mechanics of Porous Continua*. New York: Wiley, 1995.

[17] T. Okano, Y. H. Bae, and S. W. Kim, "Temperature responsive controlled drug delivery," *Pulsed and Self-Regulated Drug Delivery*, pp. 17–46, 1990.

[18] T. Miyata, N. Asami, and T. Uragami, "A reversible antigen-responsive hydrogel," *Nature*, vol. 399, pp. 766–769, 1999.

[19] E. Ruckenstein and V. Sasidhar, "Acid generating immobilized enzymic reactions in porous media-activity control via augmentation of proton diffusion by weak acids," *Chem. Eng. Sci.*, pp. 1185–1200, 1984.

[20] N. A. Peppas and L. Brannon-Peppas, "Equilibrium swelling of pH-sensitive hydrogels," *Chem. Eng. Sci.*, pp. 715–722, 1989.

[21] T. Wallmersperger, B. Kroplin, J. Holdenried, and R. W. Gulch, "A coupled multi-field-formulation for ionic polymer gels in electric fields," in *SPIE 8th Annu. Symp. Smart Struct. Mats.*, vol. 4329, Mar. 2001, pp. 264–275.

[22] E. P. Popov, *Engineering Mechanics of Solids*. Englewood Cliffs, NJ: Prentice-Hall, 1990.

[23] R. H. Liu, Q. Yu, and D. Beebe, "Fabrication & characterization of hydrogel-based micro-valves," *J. Microelectromech. Syst.*, vol. 11, no. 1, pp. 45–53, 2002.

[24] A. Baldi, Y. Gu, P. E. Loftness, R. A. Siegel, and B. Ziaie, "A hydrogel-actuated smart micro-valve with a porous diffusion barrier back-plate for active flow control," in *Proc. MEMS 2002*, 2002, pp. 105–108.

[25] L. Eldada, "Advances in telecom and datacom optical components," *Optic. Eng.*, vol. 40, no. 7, pp. 1165–1178, 2001.

[26] M. T. am Ende, D. Hariharan, and N. A. Peppas, "Factors influencing drug and protein transport and release from ionic hydrogels," *Reactive Polymers*, vol. 25, pp. 127–137, 1995.

[27] D. Luo, K. W. Mumford, N. Belcheva, and W. M. Staltzman, "Controlled DNA delivery systems," *Pharmaceutic. Res.*, vol. 16, no. 8, pp. 1300–1307, 1999.

[28] S. Nemat-Nasser and J. Y. Li, "Electromechanical response of ionic polymer metal composites," *J. Appl. Phys.*, vol. 87, no. 7, pp. 3321–3330, 2000.

[29] J. H. Nussbaum, Ph.D. dissertation, M.I.T., Dep. Elec. Eng. Comput. Sci., 1986.

[30] M. A. Biot, "Theory of elasticity and consolidation for a porous anisotropic solid," *J. Appl. Phys.*, vol. 26, pp. 182–192, 1955.

[31] N. R. Aluru and G. Li, "Finite cloud method: A true meshless technique based on a fixed reproducing kernel approximation," *Int. J. Numer. Meth. Eng.*, vol. 50, no. 10, pp. 2373–2410, 2001.

[32] B. H. Jo, L. M. Van Lerberghe, K. M. Motsegood, and D. J. Beebe, "Three-dimensional micro-channel fabrication in polydimethylsiloxane (PDMS) elastomer," *J. Microelectromech. Syst.*, vol. 9, no. 1, pp. 76–81, 2000.

[33] P. Y. Bruice, *Organic Chemistry*. Englewood Cliffs, NJ: Prentice Hall, 2001.

[34] G. M. Eichenbaum, P. M. Kiser, S. A. Simon, and D. Needham, "pH and Ion-triggered volume response of anionic hydrogel microspheres," *Macromolecules*, vol. 31, pp. 5084–5093, 1998.

[35] R. R. Ohs, Master thesis, Dept. General Eng., UIUC, 2001.

Sudipto K. De received the B.Tech. degree from the Indian Institute of Technology, Kharagpur, India, in 2000 and the M.S. degree from the University of Illinois at Urbana-Champaign (UIUC) in 2002, both in mechanical engineering. He is currently working toward the Ph.D. degree in mechanical engineering at UIUC.

His research interests include computational analysis and design of MEMS/Bio-MEMS and numerical methods in engineering.

N. R. Aluru (M'00) received the B.E. degree with honors and distinction from the Birla Institute of Technology and Science (BITS), Pilani, India, in 1989, the M.S. degree from Rensselaer Polytechnic Institute, Troy, NY, in 1991, and the Ph.D. degree from Stanford University, Stanford, CA, in 1995.

From 1995 to 1997, he was a Postdoctoral Associate at the Massachusetts Institute of Technology, Cambridge. In 1998, he joined the Department of General Engineering, University of Illinois, Urbana-Champaign (UIUC) as an Assistant Professor. He is affiliated with the Beckman Institute for Advanced Science and Technology, the Department of Electrical and Computer Engineering, and the Mechanical and Industrial Engineering at UIUC. His current research interests are in the areas of computational methods, MEMS/NEMS, micro/nano fluidics, Bio-MEMS, and bionanotechnology.

Dr. Aluru received the NSF CAREER Award and the NCSA Faculty Fellowship in 1999, a CMES Distinguished Young Author Award in 2001, and a Xerox Award and a Willet Faculty Scholar Award in 2002. He is a an Associate Member of ASME.

B. Johnson received the B.S. degree in mechanical engineering from the Illinois Institute of Technology, Urbana-Champaign, in 2000. He is currently pursuing the M.S. degree in biomedical engineering at the University of Wisconsin at Madison.

His research includes work in the mechanical characterization of responsive hydrogels used in microfluidic devices.

W. C. Crone received the B.S. degree in engineering mechanics from the University of Illinois, Urbana-Champaign, in 1990, the M.S. degree in engineering from Brown University, Providence, RI, in 1991, and the Ph.D. degree from the University of Minnesota, Minneapolis, in 1998.

She is an Assistant Professor in the Department of Engineering Physics at the University of Wisconsin at Madison with affiliate faculty positions in the Department of Biomedical Engineering and the Materials Science Program. During her graduate work at the University of Minnesota, she held an Engineering Dissertation Fellowship from the American Association of University Women (1997–1998), Amelia Earhart Fellowship from Zonta International (1995–1997), and Graduate School Fellowship (1994–1995). From 1993 to 1994, she held the position of Assistant to the Dean and Director of the Program for Women in the Institute of Technology at the University of Minnesota. From 1992 to 1993, she was an Engineer with GUIDANT Cardiac Pacemakers, Inc., St. Paul, MN. In 1992, she held a Rotary Foundation Fellowship for Study Abroad and attended the University of New South Wales, Australia. In 1990, she held the GE Foundation Fellowship and University Scholarship at Brown University. Her research investigates the mechanics of modern materials, using experimental solid mechanics techniques to understand material behavior. She has conducted research on shape memory materials, metallic single crystals, and biomaterials with specific emphasis on reversible phase transforming behavior, plastic deformation, and fracture in these materials.

Dr. Crone is a Member of ASME and the ASEE. She is the Vice- Chair and Co-Founder of the MEMS and Nanotechnology Technical Division of the Society for Experimental Mechanics.

David J. Beebe (S'89–M'95) received the B.S. , M.S., and Ph.D. degrees in electrical engineering from the University of Wisconsin at Madison, in 1987, 1990, and 1994, respectively.

He is an Associate Professor in the Department of Biomedical Engineering at the University of Wisconsin at Madison with joint appointments in Electrical and Computer Engineering and Mechanical Engineering. From 1996 to 1999, he was an Assistant Professor in the Department of Electrical and Computer Engineering and an Assistant Research Professor in the Beckman Institute for Advanced Science and Technology at the University of Illinois at Urbana-Champaign. From 1994 to 1996, he was an Assistant Professor at Louisiana Tech University. From 1991 to 1994, he was an NIH Biotechnology Predoctoral Trainee. During that time, he spent three months at Medtronic developing hemodynamic sensing concepts. He was an electrical engineer for Kimberly-Clark Corporation from 1987 to 1989, where he lead the packaging controls group. He has over 120 publications including four book chapters. He serves on the steering/program committees for the μTAS and Hilton Head conferences and he Co-Chairs the Annual IEEE EMBS Special Topic Conference on Microtechnology, Medicine and Biology. He has served on many government advisory panels including the NRC's National Nanotechnology Initiative review panel. He is a Co-Founder of Vitae LLC that is commercializing microfluidic systems for assisted reproduction and consults for various companies in the biotech and microfluidics field. He is an inventor on three issued patents and ten pending patent applications. He has broad interests in biomedical instrumentation and the development and use of microfabricated devices for applications in medicine and for the study of biology. His current interests include technology development for the handling and analysis of biological objects, development of nontraditional autonomous micro fluidic devices and systems, the study of cell and embryo development in microenvironments, development of electrostatic and electrocutaneous haptic displays, and the development of tactile sensors.

J. Moore received the B.S. degree in chemistry and the Ph.D. degree in materials science from the University of Illinois, Urbana-Champaign, in 1984 and 1989, respectively.

He was an NSF Postdoctoral Fellow at Caltech and an Assistant Professor at the University of Michigan, Ann Arbor, before joining the faculty in 1993. He is also an Associate Editor for the *Journal of the American Chemical Society* and a faculty member of the Beckman Institute, where he is the Co-Chairman of the Molecular and Electronic Nanostructures Main Research Theme.